Proc. of the 9th Intl. Conf. of Asian Society for Precision Engg. and Nanotechnology (ASPEN 2022)
15–18 November 2022, Singapore. Edited by Nai Mui Ling Sharon and A. Senthil Kumar
doi://10.3850/978-981-18-6021-8_OR-14-0040

Feasibility study on laser fusion cutting of ultra-thin glass (UTG) aimed for defect-free, molten edge formation

Sho Itoh[1,#], Naoto Nagano[1], Shun Obuchi[1], Souta Matsusaka[1] and Hirofumi Hidai[1,2]

1 Department of Mechanical Engineering, Chiba University, 1-33 Yayoi-cho, Inage-ku, Chiba-shi, Chiba, 263-8522, Japan
2 Molecular Chirality Research Center, Chiba University, 1-33 Yayoi-cho, Inage-ku, Chiba-shi, Chiba, 263-8522, Japan
Corresponding Author / Email: ittosyo@chiba-u.jp, TEL: +81-43-290-3224

KEYWORDS: Laser fusion cutting, Ultra-thin glass, Bending strength

Ultra-thin glass (UTG) with a thickness of less than 200 μm is a promising material because UTG haves excellent lightweightness and flexibility, originated from its thinness, as well as typical glass characteristics. Thus, a variety of new applications has been proposed and developed. One of the challenges of UTG application, which is also caused by its thinness, is the difficulty of processing, including cutting, drilling, and other micromachinings after UTG is formed. For example, defects are created around the edge during a typical cutting process and will drastically reduce the edge strength. Therefore, an alternative cutting process is still required to promote UTG to be utilized for manufacturing. The authors identify the technical gap here and focus on the potential of laser fusion cutting, which induces molten edges where a higher edge strength is expected. In this study, the experimental setup of laser fusion cutting is designed specifically to cut UTG. Then, the key parameters, such as laser powers, scanning speeds, and assist air angles, are identified, and the influence on the edge shape is elucidated. Finally, the method to reduce the thermal stress caused by laser irradiation is proposed and demonstrated together with the quantitatively estimated thermal stresses.

NOMENCLATURE

θ = assist air angle (pitch)
ψ = assist air angle (yaw)
σ_{max} = maximum bending stress
E = Young's modulus
t = sample thickness
D = breaking height

1. Introduction

Glass forming technology has been advanced remarkably, then ultra-thin glass (UTG, usually having a thickness of less than 200 μm) with a large area has been commercialized. Utilizing the flexibility of UTG, a wide range of new applications has been proposed, such as ultra-thin foldable display [1], ultra-thin OLED lighting [2], flexible solar cells [3], and ultra-thin microfluidic chips [4]. However, the industrial application of UTGs is limited only to some areas and has not progressed well to the best of the authors knowledge. The authors consider that one of the technical barriers is the difficulty of processing UTGs due to the thinness leading to the breakage even if defects are small. For example, scribing and breaking via scribing wheel [5] is a typical cutting process to cut thin glass substrates. However, in the case of UTG, the defects such as radial cracks will cause breakage. Laser thermal cutting has been widely used to cut UTG. However, even if the cutting quality is good, defects may be created during its post-separation process because the process mechanism is based on crack propagation without kerf loss [6]. Scribing via ultra-short pulsed laser, or so-called filamentation has been developed [7] and applied to some types of commercialized glass, such as chemically strengthened glass. However, this process is based on without kerf loss, leading to the same separation problem as shown in laser thermal cutting. Therefore, the author considers that further development in cutting UTGs is still required.

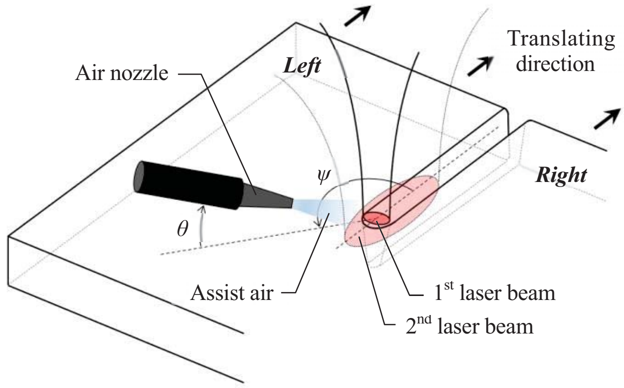

Fig. 1 Schematic of the experimental setup for laser fusion cutting of UTG

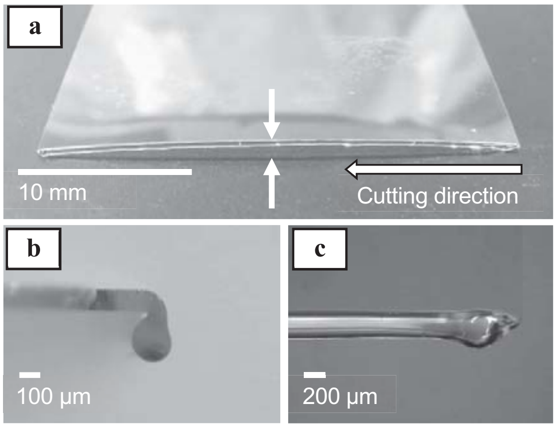

Fig. 2 Photographs of (a) overview of the cut UTG (bending height is arrowed in the image), (b) sectional view of the cut UTG, (c) magnified view near the cutting start point

To overcome these drawbacks, the authors focus on the potential of laser fusion cutting, typically used in cutting metals. When it comes to cutting glass, the application of laser fusion cutting is only limited to cutting fused silica, as the thermal expansion coefficient is low, resulting in less thermal stress compared with the case of other commercialized glasses. However, the authors focus on the thinness of UTG and the possibility that time to heat penetration is less, leading to the potential to reduce thermal stresses compared with the thicker glass plates. Also, laser fusion cutting will create a molten edge resulting in the expected rounded, defect-free surface. In this study, the laser fusion cutting setup was designed specifically to cut UTGs. Then, the parametric study was conducted, including identifying key parameters. Finally, the residual stress and edge strength were estimated, and the reasons for the values were discussed.

2. Experimental

Fig. 1 shows the experimental setup for laser fusion cutting of UTG. A CO_2 laser beam ("1st laser beam") was emitted from an oscillator (C-40, Coherent Inc.) and delivered through a pair of lenses to control the beam spot size at the UTG surface. The spot size is ~100 μm estimated via measured value using the knife-edge method at the beam expanded location before the focal lens with a focal length of 100 mm. UTG (Willow, Corning Inc.) was put on a mechanical stage and translated into a cutting direction. Assist air was supplied through a nozzle onto the molten spot on the workpiece. The distance between the nozzle tip and the molten spot was 2 mm. Assist air angles (θ, ψ) were set and controlled. Assist air inlet pressure was set at 0.2 MPa. In the experiment for the reduction of the thermal stress, another CO_2 laser beam ("2nd laser beam") emitted from an oscillator (Evolution 100, Synrad Inc.) was delivered and focused through a cylindrical lens and illuminated onto the surface nearby the molten spot. The 2nd laser beam spot was elliptical with a size of 1.3 by 3.9 mm.

Separated glasses were named *Left* and *Right*, and the cut sample was analyzed using a laser microscope (LEXT OLS4000, Olympus Corp.). The residual stress was estimated using a polarization camera (Crysta PI-5P, Photron Ltd.). A universal testing machine (Instron, Instron Corp.) was used for the two-point bending test. 5 samples in each condition were evaluated, and the averaged values and the standard deviation were acquired. Mechanical scribing and breaking samples were prepared using a scribing wheel (APIO-DCWT, Mitsuboshi Diamond Industrial Co., Ltd.) for a reference bending strength value.

3. Results and discussions

3.1 Preliminary trial of laser fusion cutting of UTG

Figs. 2 show the example of the UTG sample cut using the 1st laser beam with a laser power of ~18 W. Fig. 2a shows the overview of the cut specimen, which curved upwards with a bending height of ~1 mm (arrowed in the image). The reason for the upward curvature is considered because the irradiation side became compressive as the wider area was heated and quenched, and the back side became tensile stress to compensate for the stress balance. Then the sample was curved so that these stresses were relaxed. Therefore, it can be concluded that thermal management is required when cutting UTGs by this method. Fig. 2b represents a sectional view of the cut edge. The glass edge was drooped down, and the tip was swollen. The thickness of the glass edge became 2–3 times larger than the other parts. Compared with metals, glass viscosity gradually changes depending on the temperature. Thus, controlling the assist air blowing area is essential to reduce the increase in the glass edge thickness. In the case of Fig. 2b, the wider area was illuminated by the laser. Then it was considered that the excessive amount of molten glass led to a swollen edge formed when the temperature decreased. Fig. 2c represents a side view of the cut sample nearby the cutting start point. Only at the cutting start point, the edge became an irregular shape, which was probably caused by heat accumulation at the corner area.

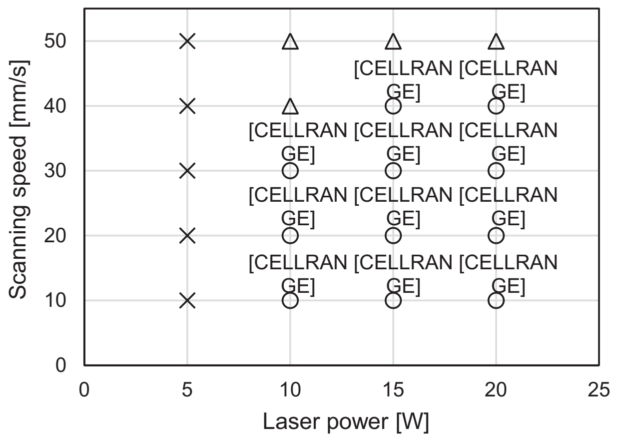

Fig. 3 Influence of laser power and scanning velocity on cutting results. When UTG was cut entirely, partially, and could not be cut in all areas, the graph was plotted as a circle, triangle, and times symbol, respectively

However, other than that portion, a clear molten surface was formed. From these results, it can be concluded that (1) thermal management and (2) edge shape control is inevitable to improve the quality of the cut sample.

3.2 Key parameters and the influences on cutting results

First, the cutting process window was examined in terms of input energy. The assist air angle was set at $(\theta,\ \psi) = (45°,\ -180°)$. Fig. 3 shows the influence of cutting speed and laser power. Each point was depicted as a circle, triangle, and times symbol when the glass was cut entirely, partially, and could not be cut in all areas, respectively. Also, the edge thickness value (depicted in Fig. 4 shown later) in a unit of µm was added together on each plot when the glass was entirely cut. Compared with the same scanning speed (E.g., 10 mm/s), edge thickness decreased along with laser power. Also, compared with the same laser power (E.g., 20 W), the edge thickness decreased when the scanning speed increased. These behaviors can be explained by the amount of heat dissipated into the surroundings. If the extra heat was dissipated into the surrounded area, more area was molten, leading to the drooped edge shape.

Then, the influence of the assist air angle on edge shapes was investigated. Figs. 4 show the sectional views of glass edge cut with an assist air angle of $\psi = 0°, -90°, -180°$, while $\theta = 45°$. In the case of $\psi = 0°$, the edge part protruded into both the upper and bottom sides in the *Left* and *Right* samples. In the case of $\psi = -90°$, the edge protruded upper side slightly and drooped into the bottom side on the *Left* side, while only drooped down on the *Right* side. On the other hand, in the case of $\psi = -180°$, protrusion could not be seen, and the edge was drooped down only. The reason was considered that assist air bumped into a molten glass wall and pushed the molten glass aside. On the other hand, in the case of $\psi = -180°$, the molten glass wall was not formed.

3.3 Residual thermal stress and bending strength

Figs. 5 show an example of the retardation map of cut UTG around the cutting start point observed through the polarization camera in case (a) without and (b) with 2nd laser beam. First, the red-colored area along the cutting line can be seen. This area is considered molten, and the sample thickness change leads to the retardation amount change. As arrowed in Fig. 5a, the concentrated retardation area (maximum value of ~8 nm) near the cutting start area can be seen. The location corresponds to the origin of the cracking when the cut glass is spontaneously broken after time passed. With 2nd laser beam, the retardation value was averagely decreased with the reduced maximum retardation value of ~5 nm at the corner, as

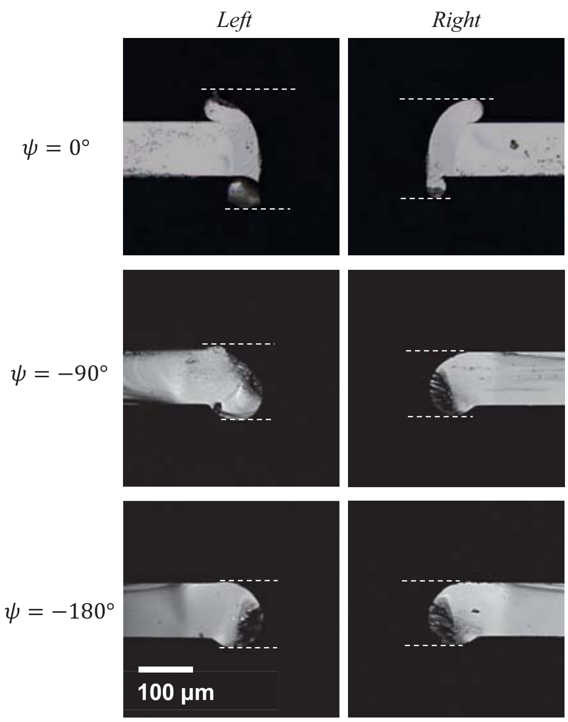

Fig. 4 Micrographs of the edge shapes in *Left*- and *Right*-side glasses, when $\psi = 0°, -90°, -180°$, while $\theta = 45°$

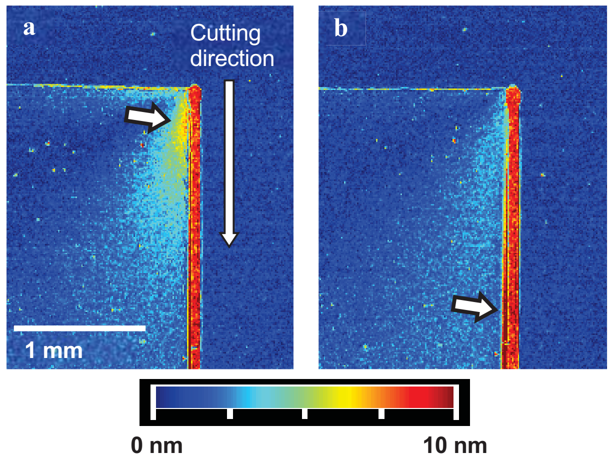

Fig. 5 Retardation map of cut UTG around the cutting start point observed via polarization camera. (a) Without and (b) with 2nd laser beam.

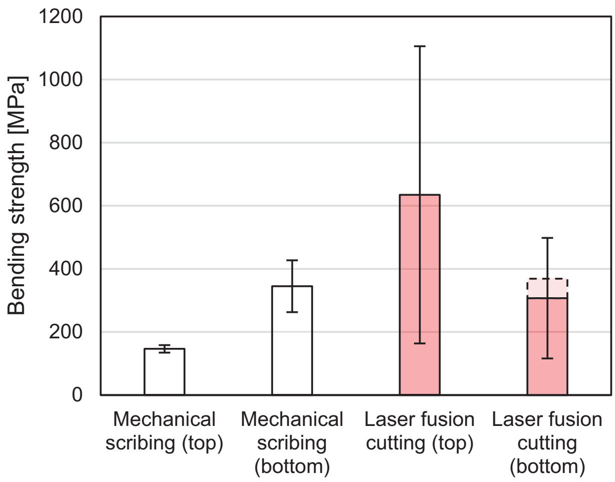

Fig. 6 Compared values of the two-point bending strength on laser fusion cutting and mechanical wheel scribing and breaking methods

shown in Fig. 5b. By adding 2nd laser beam, the residual thermal stress is lowered. The evidence is that the sample bending height value defined in Fig. 2a was decreased from ~0.9 mm to ~0.6 mm, and the spontaneous breaking did not occur in the samples prepared with 2nd laser beam. In Fig. 5b, on the other hand, a slight color change can be seen parallel to the cutting line (arrowed in the figure). The reason is that by adding 2nd laser beam, the molten pool profile changed, leading to an expanded area of the molten part. Further extensive research, including the study on the influence of relative location of 1st and 2nd laser beam, should be performed.

Regarding the evaluation of edge strength, a two-point bending test was applied. As shown in Fig. 6, the average measured breaking stresses were 147 MPa (top surface), 345 MPa (bottom surface) in the case of mechanical scribing, while 635 MPa (top surface) and 307 MPa (bottom surface) in the case of laser fusion cutting. It also should be noted that the data variation was more significant in laser fusion cutting samples than in mechanical scribing samples. Here, the reason for these breaking stress values is discussed. One of the primary factors influencing the edge strength will be edge thickness. In this two-point bending test, the applied bending stress was evaluated by using the following equation [8]

$$\sigma_{max} = 1.198(Et/D - t). \quad (1)$$

Here, we assumed the uniform edge thickness value, corresponding to the substrate thickness value of 0.1 mm. However, the sample edge was drooped down with the edge thickness value of ~0.12 mm, as shown in Fig. 4. Then, regarding the calculated edge strength of the bottom surface, the 1.2 times larger stress may be applied to the sample (shown in a broken bar in Fig. 6). Thermal stress will also influence the edge strength. As written in Section 3.1, the top surface has compressive stress while tensile stress is on the bottom surface of the cut samples. However, the 2nd beam was applied to reduce the thermal stress, so not much difference is expected. Therefore, another factor might influence the edge strength. For example, the glass particles from a molten spot that deposit onto the surface may weaken the strength.

4. Conclusions

This research studied the feasibility of laser fusion cutting of UTGs. The key parameters, such as laser power, scanning speed, and assist air angle, were identified to control the edge shape. By introducing 2nd laser beam, the stress value was changed, then spontaneous breaking was eliminated. The average edge strengths achieved were 635 MPa (top surface) and 307 MPa (bottom surface), while more significant data variation was observed than in the case of mechanical scribing and breaking.

ACKNOWLEDGEMENT

The authors gratefully acknowledge the financial support of JSPS KAKENHI (Grant Number JP22K14157) and the technical support of Photonic Lattice Inc.

REFERENCES

1. Ha, M.H., Choi, J.K., Park, B.M. and Han K.Y., "Highly flexible cover window using ultra-thin glass for foldable displays," J. Mech. Sci. Technol., Vol. 35, No. 2, pp. 661-668, 2021.
2. Wang, D., Hauptmann J., May, C., Hofstetter, Y.J., Vaynzof, Y. and Müller, T., "Roll-to-roll fabrication of highly transparent Ca:Ag top-electrode towards flexible large-area OLED lighting application," Flex. Print. Electron., Vol. 6, No. 3, pp. 035001, 2021
3. Kim, D., Shin, S.S., Lee, S.M., Cho, J.S., Yun, J.H., Lee, H.S. and Park, J.H., "Flexible and Semi-Transparent Ultra-Thin CIGSe Solar Cells Prepared on Ultra-Thin Glass Substrate: A Key to Flexible Bifacial Photovoltaic Applications," Adv. Funct. Mater., Vol. 30, No. 36, pp. 2001775, 2020.
4. Yalikun, Y., Hosokawa, Y., Iino, T. and Tanaka, Y., "An all-glass 12 μm ultra-thin and flexible micro-fluidic chip fabricated by femtosecond laser processing," Lab on a Chip, Vol. 16, No. 13, pp. 2427-2433, 2016.
5. Tomei, N., Murakami, K., Fukunishi, T., Yoshida, S. and Matsuoka, J., "Direct observation of crack propagation in a liquid crystal display glass substrate during wheel scribing," Int. J. Appl. Glass Sci., Vol. 9, No. 1, pp. 105-113, 2018.
6. Yahata, K., Ohmura, E., Shimizu, S. and Murakami, M., "Clarification of crack curvature mechanism and estimation of crack shape in laser scribing of glass," Rev. Laser Eng., Vol. 20, No. 1, pp. 46-53, 2012.
7. Shin, H. and Kim, D., "Strength of ultra-thin glass cut by internal scribing using a femtosecond Bessel beam," Opt. Laser Technol., Vol. 129, pp. 106307, 2020.
8. Gulati, S. T., Westbrook, J., Carley, S., Vepakomma, H., and Ono, T., "Two Point Bending of Thin Glass Substrate," SID Symp. Dig. Tech. Pap., Vol. 42, No. 1, pp. 652-654, 2011.